Journal of Nuclear Materials 635 (2027) 157203

Contents lists available at ScienceDirect

Journal of Nuclear Materials

journal homepage: www.elsevier.com/locate/jnucmat

Quantitative imaging of hydrogen in zirconium alloy cladding by Laser Induced Breakdown Spectroscopy

S. Guilbert [a,*], L. Jolivet [b], A.M. Kpemou [a], V. Motto-Ros [b,c], M. Grosse [d], F. Trichard [b]

[a] ASNR\DiRES\SEREX\LE2M, B.P.3, 13115 Saint Paul lez Durance, France
[b] ABLATOM S.A.S., 62 Bd Niels Bohr, 69100 Villeurbanne, France
[c] Institut Lumière Matière, UMR5306, Univ. Lyon 1-CNRS, Université de Lyon, 69622, Villeurbanne, France
[d] Karlsruhe Institute Für Technologie (KIT), P.O. Box 3640 D, 7602, Karlsruhe, Germany

HIGHLIGHTS

- Quantitative LIBS methodology for H mapping in Zr alloys with 12 μm spatial resolution.
- Excellent correlation with neutron imaging, confirming the method's reliability.
- Minimal matrix effects and stable measurements (repeatability/reproducibility).
- Fast, accessible, and high-performance solution for H mapping in Zr alloys.

ARTICLE INFO

Dataset link: Hydrogen quantitative mapping by LIBS (Original data)

Keywords:
Hydrogen
μ-LIBS imaging
Fuel cladding
Neutron Imaging
Zirconium
LOCA

ABSTRACT

Hydrogen in solids is of high importance in several industries as it may induce embrittlement or stress in metallic materials. In zirconium-based nuclear fuel claddings, assessing its concentration and distribution at micro- and macro-scales is critical to understanding hydrogen uptake and embrittlement mechanisms. Despite its importance, hydrogen remains one of the most challenging elements to quantify and spatially map in solids due to its low atomic number, high mobility, susceptibility to contamination, and limited availability of spatially resolved analytical techniques. This paper presents a methodology for quantitative hydrogen analysis in zirconium alloys using Laser-Induced Breakdown Spectroscopy (LIBS), combining atmospheric-pressure operation, rapid acquisition, and micrometric spatial resolution. To ensure reliable LIBS-based hydrogen quantification, the methodology focused on the control of sample preparation, ambient hydrogen contribution, signal stability, and calibration robustness. Hydrogen calibration curves were established using hydrogen-charged zirconium alloy standards covering 12–4100 wppm. After optimization, a linear response between the H I 656.28 nm emission line and hydrogen concentration was obtained, with excellent linearity ($R^2 = 0.99$) and an estimated detection limit lower than 100 wppm. Repeatability and reproducibility studies demonstrated robust measurement stability, while the use of both Zircaloy-4 and $M5_{Framatome}$ alloys confirmed limited matrix effects under the selected conditions. Hydrogen maps acquired at 12 μm spatial resolution on steam-oxidized cladding revealed heterogeneous distributions consistent with oxidation-induced microstructural transformations. Quantitative comparison with Neutron Imaging showed excellent agreement, confirming the validity of LIBS for quantitative hydrogen mapping and highlighting its potential as an accessible alternative.

1. Introduction

Hydrogen in solids is of high importance in several industries, including steel, high-purity metals, hydrogen storage materials and alloys, as it may induce embrittlement or stress in the material. During normal operation in a nuclear reactor, fuel cladding is corroded by the water coolant and gradually picks up hydrogen, up to values as high as 600–700 wppm depending on the alloy. Once absorbed by zirconium alloys, hydrogen may dissolve interstitially and then precipitate as zirconium hydrides when the local solubility limit is exceeded.

* Corresponding author.
E-mail address: severine.guilbert@asnr.fr (S. Guilbert).

https://doi.org/10.1016/j.jnucmat.2026.157203
Received 16 July 2026; Accepted 5 October 2026
Available online 31 October 2026
0022-3115/© 2026 The Authors. Published by Elsevier B.V. This is an open access article under the CC BY license (http://creativecommons.org/licenses/by/4.0/).

Furthermore, hydrogen is highly mobile in the cladding, and its mobility is influenced by concentration, stress and temperature gradients, leading to changes in hydrogen distribution and local maxima [1]. Cladding may also pick up hydrogen when exposed to steam at high temperature during Loss Of Coolant Accident (LOCA), after ballooning and bursting. This hydrogen pickup, called secondary hydriding, results from steam ingress through the burst into the gap between the fuel pellets and the cladding inner surface and may lead to hydrogen pickup ranging from 1000 to 4000 wppm [2,3]. Hydrogen stabilizes the high-temperature β-Zr phase and concentrates into the prior-β region during cooling, leading to very heterogeneous hydrogen distribution through the cladding wall thickness. Significant azimuthal and axial hydrogen gradients were thus observed near the burst [2–4]. Hydrogen redistribution during normal operation and secondary hydriding both cause local increases in hydrogen/hydride concentration. The hydrides are brittle compared with the zirconium matrix, and their morphology, orientation and local density can strongly affect ductility and fracture resistance. An average measurement of hydrogen content is therefore useful for total hydrogen inventory, but it cannot by itself describe the local fields that control post-quench embrittlement and failure initiation.

Hydrogen is one of the most difficult elements to quantify in solids. Because it has only one electron and no deep inner electronic shell, it cannot be measured by several common material characterization techniques used for heavier elements, such as X-ray fluorescence, Electron Probe MicroAnalysis or electron spectroscopies, including Auger electron spectroscopy and X-ray photoelectron spectroscopy [5]. Its low atomic mass and high mobility also make sample preparation and storage important. Furthermore, adsorbed water, hydrocarbons and residual gases in vacuum systems can contribute to background signals. Quantitative hydrogen analysis therefore requires careful control of contamination, matrix effects and calibration standards.

Reported hydrogen contents are generally measured on small rings, 1 to 2 mm large, using Inert Gas Fusion technique (IGF), giving average values. Some measurements are also obtained through Neutron Imaging (NI) [2,3,6] or Elastic Recoil Detection Analysis (ERDA) [4,7].

The principles of NI have already been described in [6,8]. This technique can provide non-destructive mapping of hydrogen with spatial resolutions of ~20–25 μm at lowest and minimal concentrations of 100 wppm for ex-situ and ~30 wppm for in-situ measurements [6,8]. The method has to be calibrated using specimens preloaded with hydrogen for ex-situ experiments. For in-situ measurements, the correlation between the hydrogen concentration and the macroscopic neutron cross-section is determined by isothermal experiments at various temperatures and hydrogen concentrations [9]. Of course, this technique requires a cold neutron facility.

ERDA can also provide non-destructive mapping of hydrogen with a spatial resolution of $\sim 3 \times 8\ \mu m^2$ [4]. This technique uses a 3 MeV $^4He^+$ beam, which is focused on the sample surface with a 15° grazing angle. Protons ejected by elastic scattering are collected with a detector placed symmetrically, with a 15° grazing angle. ERDA has the advantage of not requiring calibration, and the bulk contribution can be isolated from the surface signal by depth resolution of the spectra. The sensitivity for hydrogen is approximately 100 wppm. More recently, the resonant $^1H(^{15}N,\alpha\gamma)^{12}C$ reaction has also proven to be suitable for hydrogen mapping in titanium [10]. However, both ion beam techniques require a Van de Graaff accelerator.

Secondary ion mass spectrometry (SIMS), although not as commonly employed as the two other techniques for hydrogen measurements in zirconium alloys [11], is known for its capabilities in elemental and isotopic analysis, as well as for providing surface distributions, depth profiles, and 3D distributions of elements, isotopes and compounds at micro- and nano-scales [12,13]. However, quantitative analysis of the hydrogen content in a sample can be challenging due to the need for calibration or for accounting for possible matrix effects and ion yield-to-concentration nonlinearities. Especially in the case of metallic samples, hydrogen analysis may be affected by high mobility of hydrogen in metals and desorption due to ultra-high vacuum or its segregation on a surface, as well as by the adsorption of hydrogen-containing molecules from the residual vacuum in a spectrometer chamber [14,15].

Other techniques can also be considered, such as Thermal Desorption Spectrometry (TDS), closely related to IGF, or Glow Discharge Optical Emission Spectroscopy (GDOES) and Glow Discharge Mass Spectrometry (GDMS), which are useful for depth profiling but not for local mapping [5].

While highly powerful, these reference techniques, including inert gas fusion, neutron imaging, micro-ERDA and SIMS, either provide average bulk measurements, or require large-scale facilities or operate under high-vacuum conditions. In addition, spatial resolution is often limited to several tens of micrometers, except for SIMS, and acquisition times remain relatively long for large-area mapping. Consequently, there remains a strong need for analytical methods combining quantitative capability, high spatial resolution, rapid acquisition, and broad accessibility.

How, then, can micrometer-scale hydrogen analysis be achieved without the constraints of large-scale facilities or high vacuum? In this context, Laser-Induced Breakdown Spectroscopy (LIBS) appears as a promising alternative. LIBS is based on the interaction of a pulsed laser beam with the surface of the sample and on the analysis of the subsequent light emission from the induced plasma. The emitted spectrum is characteristic of the elements present in the ablated material. LIBS can operate at atmospheric pressure, requires limited sample preparation, and enables rapid elemental analysis over large sample surfaces. Its capacities for quantitative analysis have been demonstrated in various fields of application [16–19].

Hydrogen measurements in fuel cladding by LIBS have been extensively studied [7,20–23]. These studies focused mainly on the determination of optimum experimental conditions for hydrogen measurement, including laser parameters, detection conditions and surrounding atmosphere, often with large beam diameters. The linearity between emission intensities and hydrogen contents in Zircaloy-4 was also demonstrated [22,23], and first hydrogen LIBS maps in $M5_{Framatome}$ cladding were presented in [7].

However, hydrogen analysis by LIBS also presents specific analytical challenges. Unlike most metallic elements, hydrogen provides only a limited number of exploitable emission lines, among which the H I 656.28 nm transition is generally the most intense and practical for quantitative analysis. Furthermore, the measured signal may originate not only from hydrogen contained in the material but also from adsorbed water molecules, ambient humidity and surface contamination. Variations in plasma temperature and electron density may also strongly affect the hydrogen emission intensity, making quantitative measurements particularly sensitive to experimental fluctuations.

As for other spectroscopic techniques, matrix effects remain an important aspect in quantitative LIBS analysis. Variations in alloy composition may influence laser–matter interaction and plasma properties, potentially affecting emission intensities and calibration robustness. Consequently, the transferability of a calibration strategy between different zirconium alloy grades must be carefully assessed for quantitative hydrogen measurements.

While previous studies have demonstrated the feasibility of hydrogen quantification in zirconium alloys, quantitative high-resolution hydrogen mapping remains comparatively less explored, particularly in the context of industrial applications requiring robust calibration procedures and validated measurement protocols. The present work therefore aims to develop and assess a LIBS methodology for quantitative hydrogen mapping in zirconium alloy cladding with a spatial resolution of 12 μm. Particular attention is paid to sample preparation, repeatability, long-term reproducibility, ambient hydrogen contribution, calibration robustness and matrix effects. Finally, LIBS hydrogen maps are compared with Neutron Imaging data in order to evaluate the validity of the approach and its potential for industrial

hydrogen analysis.

2. LIBS principles

2.1. General principles of LIBS

The Laser Induced Breakdown Spectroscopy is based on the interaction of a pulsed laser beam onto the surface of the sample leading to the formation of a transient plasma through laser ablation of the material [24–26]. The plasma contains excited atoms, ions and electrons originating from the ablated material. During its expansion and cooling, these species emit characteristic radiation that allows elemental identification and quantification. The emitted spectrum consists of discrete atomic and ionic emission lines superimposed on a transient continuum background. The plasma lifetime typically ranges from sub-microseconds to several microseconds. Time-resolved detection is generally used to optimize signal-to-background ratio. Plasma properties depend on laser parameters, surrounding atmosphere and material composition, which makes signal stability a critical aspect for quantitative analysis Hydrogen analysis by LIBS presents specific challenges. Due to its low atomic mass and high mobility, hydrogen may originate not only from the bulk material but also from adsorbed water molecules on the surface or from ambient humidity [22,23]. Moreover, only one intense atomic emission line (H I 656.28 nm) is generally exploitable in metallic systems, making measurement particularly sensitive to plasma fluctuations and background contribution. These intrinsic limitations require careful optimization of both sample preparation and experimental conditions.

An advantage of LIBS is that it can be performed at atmospheric pressure.

2.2. Specific challenges of hydrogen measurements by LIBS

Hydrogen analysis by LIBS presents specific challenges compared with conventional elemental measurements. Unlike most metallic elements, which generally exhibit numerous emission lines distributed over a broad spectral range, hydrogen offers only a limited number of exploitable atomic transitions. Among them, the H I 656.28 nm line (Hα) is the most commonly used for quantitative analysis in metallic materials owing to its high intensity and favorable signal-to-background ratio.

The Hα line corresponds to the Balmer-α transition between the $n = 3$ and $n = 2$ energy levels of atomic hydrogen. The upper level of this transition lies approximately 12.09 eV above the ground state, while the lower level is located at 10.20 eV. Such high excitation energies imply that the population of the emitting level strongly depends on plasma thermodynamic conditions, particularly electron temperature. As a result, relatively small variations in plasma formation may induce significant fluctuations in the measured hydrogen intensity.

Hydrogen emission lines are also characterized by strong Stark broadening coefficients. Since Stark broadening is directly related to electron density, variations in plasma conditions may affect not only the emission intensity but also the spectral profile of hydrogen lines. This phenomenon is particularly pronounced for the H I 486.13 nm transition (Hβ), which exhibits a significantly larger Stark broadening coefficient than Hα. Under typical LIBS plasma conditions, the resulting linewidth may become sufficiently broad to reduce peak intensity, degrade the signal-to-noise ratio, and increase the risk of spectral overlap with neighboring emissions. Consequently, Hβ is generally less suitable for quantitative measurements, making Hα the preferred analytical transition for hydrogen determination.

In addition to these spectroscopic considerations, the measured hydrogen signal may originate from multiple sources. Besides hydrogen contained within the material itself, contributions may arise from adsorbed water molecules, polishing residues, surface contamination, or ambient humidity surrounding the plasma. Consequently, the measured hydrogen emission may contain both a material-related contribution and an environmental contribution. Unlike most metallic elements, for which background contamination is generally negligible, hydrogen measurements are particularly sensitive to such external contributions and therefore require careful control of sample preparation and experimental conditions.

Furthermore, hydrogen emission intensities are strongly dependent on plasma temperature and electron density, making quantitative measurements particularly sensitive to variations in laser energy, beam quality, focusing conditions, surface roughness, and local atmosphere. While moderate fluctuations in plasma properties may only have a limited impact on many metallic emission lines, they can lead to substantial variations in hydrogen emission intensity. Therefore, quantitative hydrogen analysis requires not only optimized acquisition parameters and calibration procedures but also a highly stable LIBS instrumentation. Laser pulse energy stability, beam-pointing stability, focus reproducibility, detector stability, and atmospheric control all become critical parameters for obtaining reliable and reproducible measurements.

For these reasons, the main challenge associated with LIBS hydrogen measurements is not the detection of hydrogen itself, but the establishment of a robust methodology capable of delivering quantitative, reproducible, and spatially resolved measurements under industrially relevant conditions. Ensuring long-term instrumental stability is therefore a prerequisite for accurate hydrogen quantification and constitutes one of the key requirements for the successful deployment of LIBS as a hydrogen mapping technique.

3. Materials and methods

3.1. Materials

The specimens used in this study were cut from low tin Stress-Relieved Annealed (SRA) Zircaloy-4 and $M5_{Framatome}$ PWR 17 × 17 industrial fuel cladding tubes, provided by AREVA-NP and FRAMATOME respectively. Composition of the alloy is given in Table 1.

These specimens were used for steam oxidation tests as well as for standard preparation.

3.2. Standard preparation

The samples for LIBS calibration were prepared in a two-step process:

1 – Hydrogen charging was performed at Ecole Centrale de Paris using 70 mm long Zry-4 cladding tubes with open ends. The tube was inserted in a tight quartz tube heated by a furnace. The quartz tube was evacuated to secondary vacuum, then pure hydrogen was admitted up to few tens of mbars at 420 °C. This temperature was chosen to avoid cladding recrystallization while permitting high hydrogen concentrations homogeneous charging. Several gas injection steps were performed keeping the sample temperature at 420 °C. After hydrogen charging, the sample was slowly cooled at 20 °C/h to form circumferential hydrides uniformly distributed across the sample thickness. Tubes were then cut into ~20 mm long segments and rings are taken at each end for hydrogen content measurements by inert gas fusion.

2 - Homogenization: samples were individually sealed under vacuum in quartz bulbs and heat treated at 500 °C for several weeks. Weight variations before and after the heat treatment were controlled to check the tightness of the bulbs. Global hydrogen content was also systematically measured by inert gas fusion after annealing.

3.3. High temperature steam oxidation

Samples presenting secondary hydriding were prepared using the protocol described in [27]. The samples consist in $M5_{Framatome}$

Table 1
Chemical composition of the Zry-4 and $M5_{Framatome}$ batch used for LIBS calibration and analysis.

	Sn	Fe	Cr (wt%)	O (wt%)	Nb (wt%)	H (wppm)
Zry-4	1.29–1.31 wt%	0.21–0.22 wt%	0.11	0.127–0.137		10
$M5_{Framatome}$	<25 wppm	345–390 wppm	<50 wppm	0.13–0.14	0.97–1.00	11

recrystallized undeformed cladding with stacked pellets inside. Porcelain pellets are used as mock–up pellets to simulate the thermal behavior of UO_2 pellets. The sample is closed at the bottom part with a Swagelok cap and top part is left open for steam transport inside the sample during the oxidation stage. The thermal transient performed in a resistive furnace consists of two phases: a first heat–up phase to reach the desired oxidation temperature (~1200 °C) and after a 5 min temperature stabilization, the isothermal oxidation stage starts by injecting steam for the cladding oxidation. During the first stage, the sample is heated without steam, and this stage allows to fill the sample with argon. A quench is performed at the end of the oxidation stage to freeze the cladding metallurgical transformations.

3.4. Sample characterizations

- Global hydrogen content measurements

The average hydrogen content of the samples is measured by inert gas fusion using a LECO OH 836 analyzer. A minimum of 3 measurements was systematically performed in order to have a good assessment of the scattering of the hydrogen contents. Calibration of the analyzer is checked regularly by analyzing a hydrogen certified reference standard. The average hydrogen content was calculated as the quadratic sum of the hydrogen standard uncertainty (8%) and the standard deviation of the sample measurements.

- Neutron imaging

Neutron Imaging (NI) was used to map the hydrogen azimuthal distribution within the cladding. The benefits of this non-destructive method for hydrogen quantification in zirconium alloys have been well documented in literature [3,8,28–31]. The combination of high total neutron cross section of hydrogen and low cross section of zirconium provides the possibility of a non–destructive, quantitative determination of hydrogen concentrations in zirconium-based alloys with a spatial resolution up to about 25 μm and a resolution of the hydrogen content up to about 50 wppm [6]. In this study, neutron imaging was performed on several azimuthal strips cut from a cladding following the oxidation stage. Neutron investigations were performed at Paul Scherrer Institute (PSI) using the BOA beamline. The strips were placed in a 60 mm x 60 mm field of view, and the measurements were performed with a 50 μm spatial resolution. A holder, made in aluminum alloy was used to hold a maximum of five strips during the measurement. The measurement was made quantitative by means of a calibration curve obtained using pre-hydrided zirconium alloys samples with well-known hydrogen content.

3.5. LIBS experimental setup

All results presented in this study were obtained using a LIBS experimental setup presented in Fig. 1 and described in detail in a previous study [32]. The selected configuration is representative of a high-performance imaging configuration that can be deployed in the ABLAXPERT™ system from ABLATOM.

A laser source was a Q-switched Nd:YAG operating at its fundamental wavelength of 1064 nm and at a repetition rate of 100 Hz (Centurion GRM, Quantel) with a pulse duration of 8 ns (full width at half maximum, FWHM). Laser output stability was monitored using a power meter positioned at the cavity exit, while a mechanical shutter controlled the delivery of pulses to the sample. The beam was vertically focused onto the alloy surface using a reflective microscope objective, with the pulse energy adjusted to 500 μJ via a computer-controlled attenuator.

A 15 × magnification objective ensured precise focusing on the

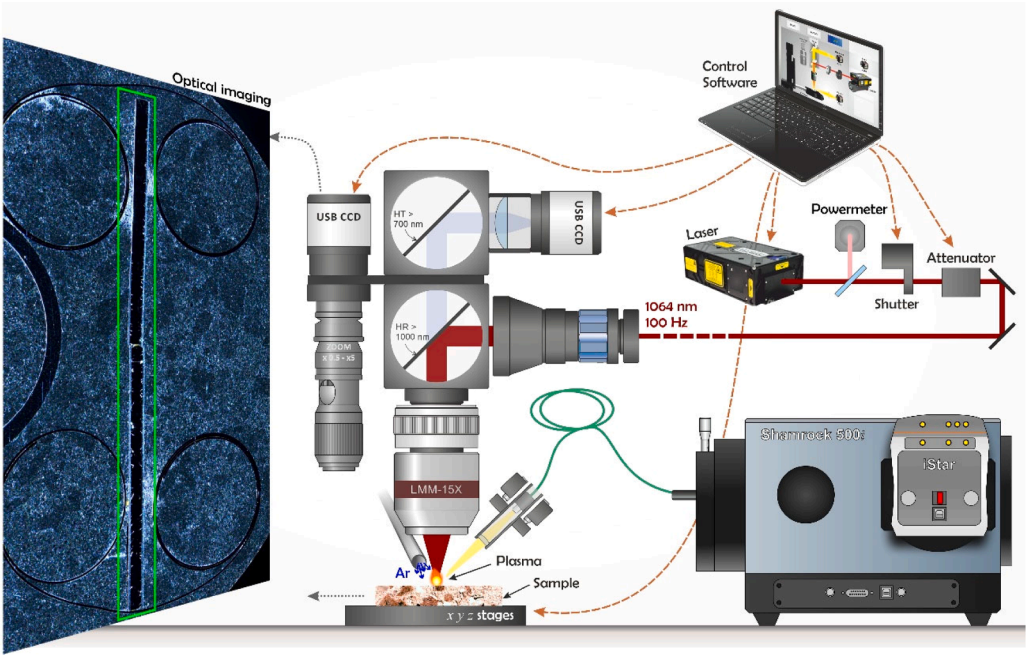


Fig. 1. LIBS instrumentation setup.

sample surface. Each sample was mounted on a motorized XYZ translation stage, enabling automated point-by-point scanning with predefined lateral spacing. During acquisition, the sample was translated line-by-line beneath the stationary laser beam to cover the region of interest. The average ablation depth per pulse, determined using a 3D optical microscope, was approximately between 8 and 10 μm. To avoid crater overlap, a lateral step size of 12 μm was employed in all measurements shown below.

Plasma emission was collected via an optical fiber and analyzed by a Czerny-Turner spectrograph (Shamrock 500, Andor Technology, Northern Ireland) equipped with intensified CCD (ICCD) camera dedicated to hydrogen detection in the visible range. Detection parameters, including gate delay, gate width, and acquisition settings, were optimized to improve the limit of detection and maximize the signal-to-noise ratio (SNR). The gate delay and gate width were set to 80 ns and 800 ns, respectively.

To maximize spectral transmission efficiency for hydrogen detection, the H I 656.28 nm line was positioned at the center of the spectrometer range. Several grating configurations were evaluated; the optimal configuration employed a 1200 lines/mm grating blazed at 300 nm, achieving high quantum efficiency while minimizing interference from minor zirconium emission lines. Under this configuration, the spectral range extended from 636.80 to 674.93 nm, with a resolution of ~0.03 nm and maximized quantum efficiency at 656 nm.

In addition to the LIBS analytical channel, the instrument is equipped with a wide-field optical imaging system allowing rapid visualization of the sample surface prior to analysis. This imaging channel provides a macroscopic view of the specimen and facilitates the identification of regions of interest, sample positioning, and definition of acquisition sequences. The optical image is used to select the areas to be mapped, optimize the analysis strategy, and verify the overall quality of the sample surface before LIBS measurements.

All experiments were performed under ambient conditions with a continuous argon flow (1.0 L/min) directed across the plasma region. This localized inerting enhanced plasma emission, improved SNR, and minimized surface contamination from redeposition of ablated material. The laser operated at a 100 Hz repetition rate, enabling acquisition of LIBS images of 2100 × 96 pixels for each sample in approximately 34 min.

For each pixel, the net intensity of a selected emission line was determined by subtracting the local background from the integrated signal within a 0.2 nm spectral window centered on the line of interest [33].

4. Results and discussions

4.1. Sample preparation

Embedding was performed prior to polishing in order to provide mechanical support to the thin cladding strips and facilitate the preparation of a flat and homogeneous surface (Fig. 2a). Such surface quality is required to ensure consistent analytical conditions during LIBS measurements. To ensure both performance and reproducibility of LIBS hydrogen measurements, the influence of the embedding material was first evaluated. Several sample preparation strategies were therefore investigated, including a black polymer resin (EPMA/SEM-compatible) and two copper-based resins (TEM-compatible). The evaluation of preparation methodology was based on two primary criteria:

(i) The prepared surface must be sufficiently flat and aligned with the laser focal plane;
(ii) the preparation process must minimize introduction of surface contamination.

The same hydrogen-homogeneous zirconium alloy standard was prepared using each method and were analyzed using the same LIBS protocol.

All embedded samples presented excellent surface quality, but LIBS analysis revealed detectable hydrogen signals originating from the embedding resins themselves. Complementary LIBS analysis of carbon and copper (Fig. 2b) confirmed that polymer resin produced the lowest redeposition on the alloy surface after polishing and LIBS ablation. Consequently, the polymer resin embedding protocol was selected for all subsequent measurements.

4.2. Short- and long-term reproducibility and sample stability

The short-term reproducibility of LIBS measurements was assessed through the hydrogen signal in order to evaluate the consistency of the measurement protocol under identical experimental conditions. Two repeated LIBS imaging experiments were performed on a single sample selected from reference standards: the H 626 wppm standard. The specimen was prepared using the optimized sample preparation protocol described in the previous section and analyzed on the same LIBS instrument under identical acquisition conditions.

To avoid potential bias from a second polishing step, the homogeneous standard was divided into two parts after preparation, as illustrated in Fig. 3. Each LIBS image was acquired on a distinct prepared

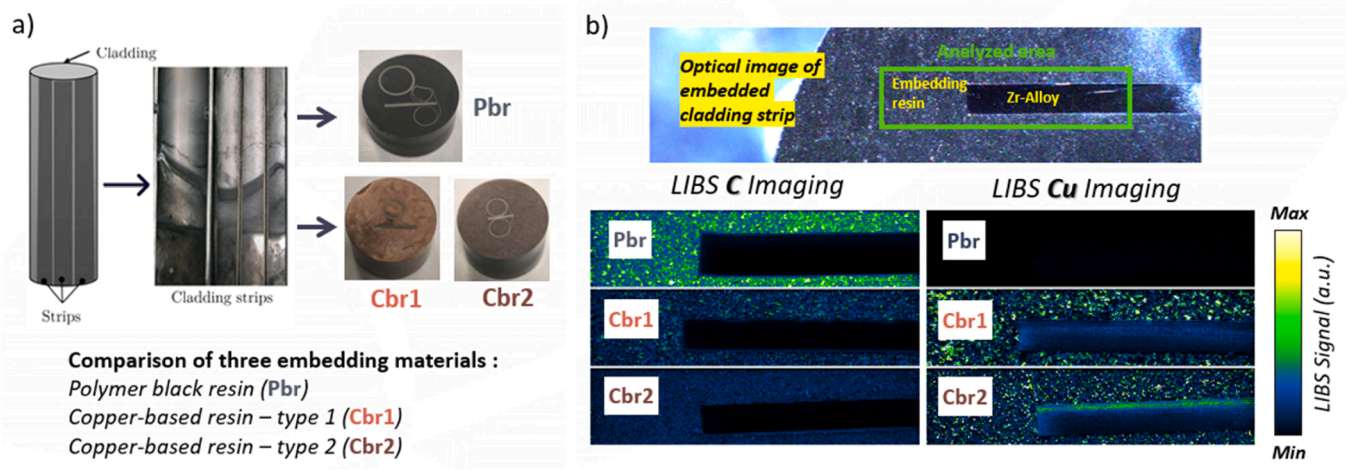


Fig. 2. Comparison of embedding materials for LIBS sample preparation: (a) Schematic representation of cladding strip preparation and embedding in three different materials prior to LIBS analysis; (b) Optical image of the analyzed surface and corresponding LIBS elemental maps used to assess possible contamination from embedding materials.

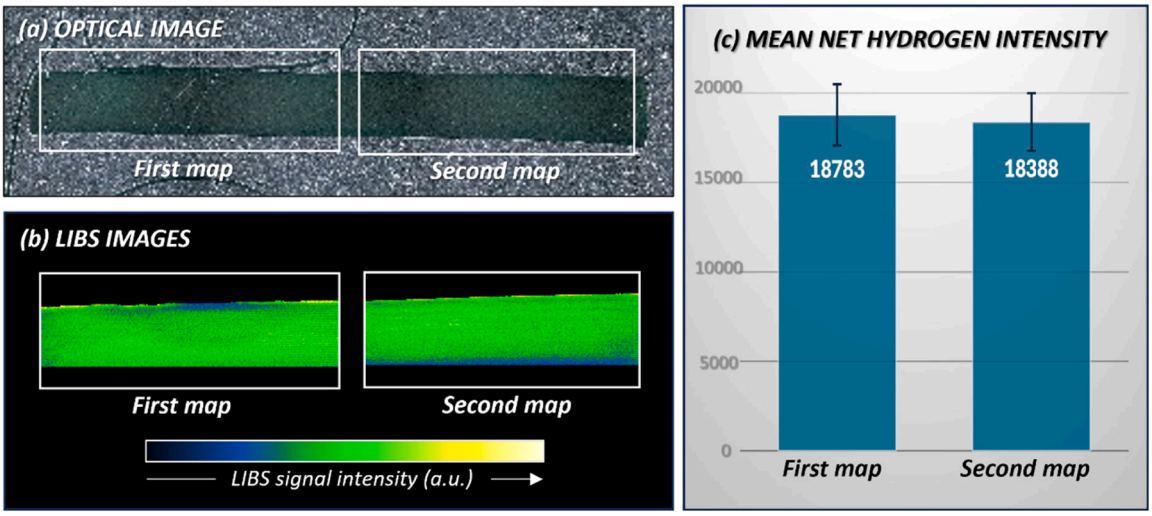


Fig. 3. Repeatability assessment: case of hydrogen (H 626 wppm standard).

area of the same specimen without repositioning the sample between the two acquisitions. The transition time between the two measurements was approximately 2 min.

Short-term reproducibility was evaluated by comparing the mean net intensity of the hydrogen reference emission line between the two LIBS images. The mean net intensity of the reference emission line was obtained by subtracting the local spectral background from the integrated signal within a narrow spectral window centered on the line of interest.

The results show good repeatability. The relative differences between the two repeated measurements were 2.15%, as illustrated in the LIBS mapping shown in Fig. 3. This result confirms that the optimized sample preparation and acquisition protocol provides consistent hydrogen signals for repeated measurements performed under the same experimental conditions.

Building on this short-term reproducibility assessment, the next step was to evaluate the reproducibility of LIBS measurements over time, i.e., the ability to obtain consistent results when the same measurement protocol is applied over different experimental sessions. The objective was to verify the absence of any measurement drift over time, which could arise from factors such as instrument stability or changes in the sample itself.

Seven LIBS imaging sequences were performed over seven consecutive days on a homogeneous reference specimen (bar-end sample) prepared according to the validated protocol described in Section 5.1. The measurements were carried out over a total period of seven days, with one LIBS imaging sequence acquired per day. The sample was divided into seven parts as illustrated in Fig. 4. Between measurement sessions, the sample was stored under ambient laboratory conditions, with the analyzed surface covered by a temporary adhesive-free protective polymer film to limit exposure to dust and humidity.

Each measurement corresponded to an imaged region of 650 × 70 pixels (45,500 pixels in total) providing a sufficiently large surface area to obtain a representative net signal value. For statistical monitoring, a control chart was constructed with the target value defined as the mean net hydrogen signal over all 7 measurements.

The control chart showed that the hydrogen signal remained stable over the seven-day measurement period, with no significant drift observed between sessions. The measured values remained close to the mean target value, indicating that the combined effects of instrumental stability, sample preparation, and sample storage did not introduce significant variability over time. These results confirm the suitability of the optimized protocol for reproducible hydrogen measurements by LIBS over multiple experimental sessions.

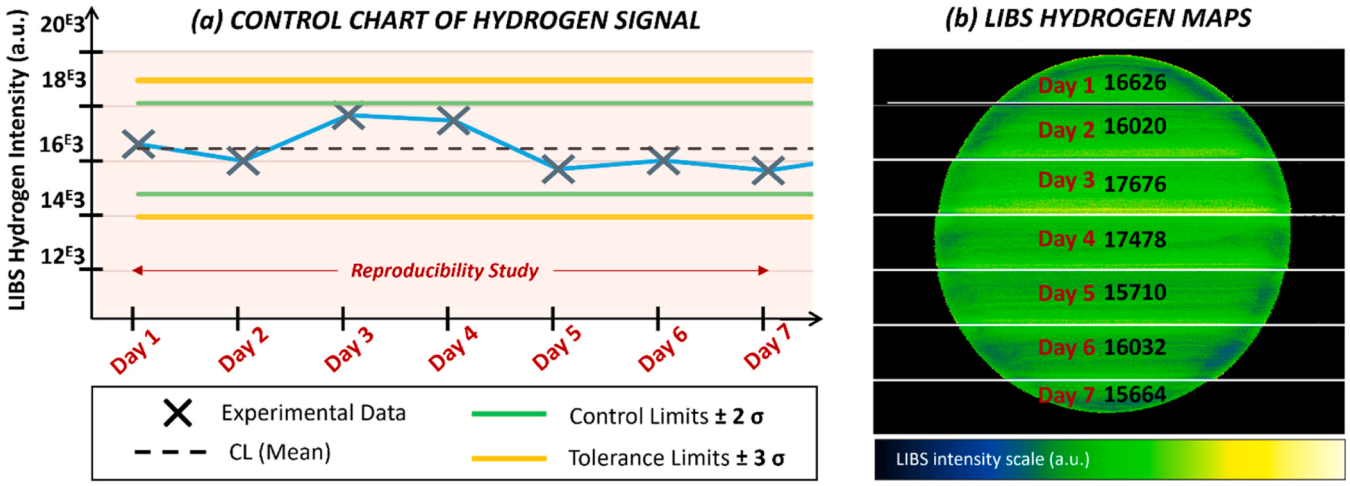


Fig. 4. Reproducibility assessment over 7 days: (a) statistical control chart of hydrogen signal and (b) associated hydrogen mapping with mean net signal for the seven measured regions.

4.3. Calibration strategy and matrix effect assessment

A calibration strategy of the LIBS signal for hydrogen quantification in Zr alloys from industrial fuel cladding tubes was established to ensure accuracy and reproducibility of the analytical results.

First, a set of synthetic calibration standards with known hydrogen contents ranging from 12 to 4107 wppm were prepared as described in 3.2. The global hydrogen content for each sample was evaluated by inert gas fusion described in 3.4 providing reference values for calibration. Two types of zirconium alloys were considered among the available standards: Zry-4 and $M5_{Framatome}$. Chemical compositions of each alloy type as well as their estimated hydrogen global content are given in Table 1. The use of two industrial Zr alloy grades also allowed the influence of possible matrix effects on hydrogen quantification to be evaluated. Although both materials are Zr-based, their alloying elements differ with Sn-based Zry-4 and Nb-based $M5_{Framatome}$ compositions. Such compositional differences may potentially affect LIBS signal response through variations in laser absorption, ablation behavior or plasma formation. Therefore, the applicability of a single calibration function to both alloy families requires experimental verification.

Second, LIBS spectra were acquired using the experimental conditions described in Sections 3.5 and 4. For each polymer resin-embedded standard, a LIBS imaging sequence consisting of 210 × 50 spectra was recorded. In order to ensure that the hydrogen signal used for calibration originated exclusively from the zirconium alloy, a binary mask was generated from the Zr emission line. This mask allowed the metallic alloy region to be distinguished from the surrounding embedding resin and only spectra associated with the alloy were retained for further processing. The resulting hydrogen maps for each standard are shown in Fig. 5. The binary mask was then applied to extract the hydrogen signal exclusively from the alloy region.

For each standard, an average hydrogen spectrum was calculated over all pixels belonging to the zirconium alloy and used to determine the calibration value. The hydrogen signal was extracted spectrum by spectrum using the procedure defined in Eq. (1) [33] which uses two spectral windows (as detailed in Fig. 6) covering, respectively, the emission line of interest and the adjacent background. The resulting effective Is intensity can thus be calculated as follows:

$$I_S = \frac{\sum_{i=1}^{n_S} I_i - n_S \overline{I_{BG}}}{n_S} \quad (1)$$

where **ns** represent the number of points in the signal window and $\mathbf{I_{BG}}$ the averaged value of the continuum.

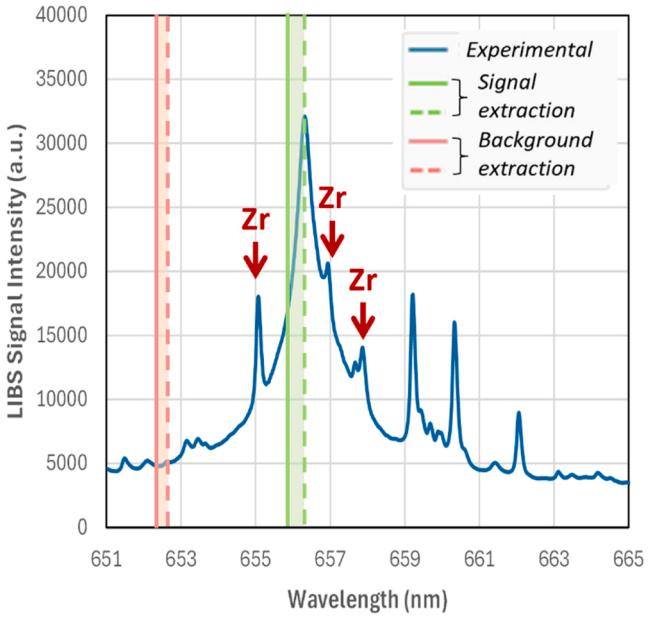


Fig. 6. Spectral windows defined respectively for the signal of the selected emission line and the averaged value of the continuum.

This signal extraction method reduces the influence of shot-to-shot fluctuations in the local continuum background, partly associated with variations in plasma formation and ablation efficiency, and therefore provides a more robust estimate of the net hydrogen emission intensity.

Calibration curves were constructed by plotting the averaged I_S-corrected hydrogen signal as a function of the known global hydrogen concentration in the alloys. The resulting calibration function exhibited a good linear correlation ($R^2 = 0.99$) as shown in Fig. 7 despite the presence of a stable offset that can be attributed to ambient hydrogen contribution. Self-absorption effects were not evidenced within the studied hydrogen range as no deviation from linearity was observed even at high concentration. In addition, independent calibration curves established separately for each alloy family also showed excellent linearity, with correlation coefficients of $R^2 = 0.99$ for Zry-4 and $R^2 = 0.96$ for $M5_{Framatome}$ standards. No significant deviation in slope or systematic alloy-dependent behavior was observed between the two alloy families under the selected experimental conditions. These results

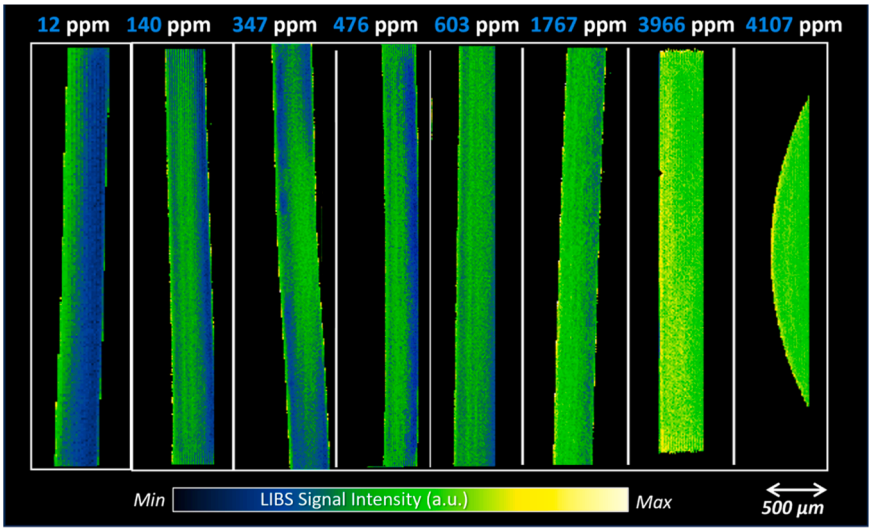


Fig. 5. LIBS H mapping of Zr alloys strips used as standards.

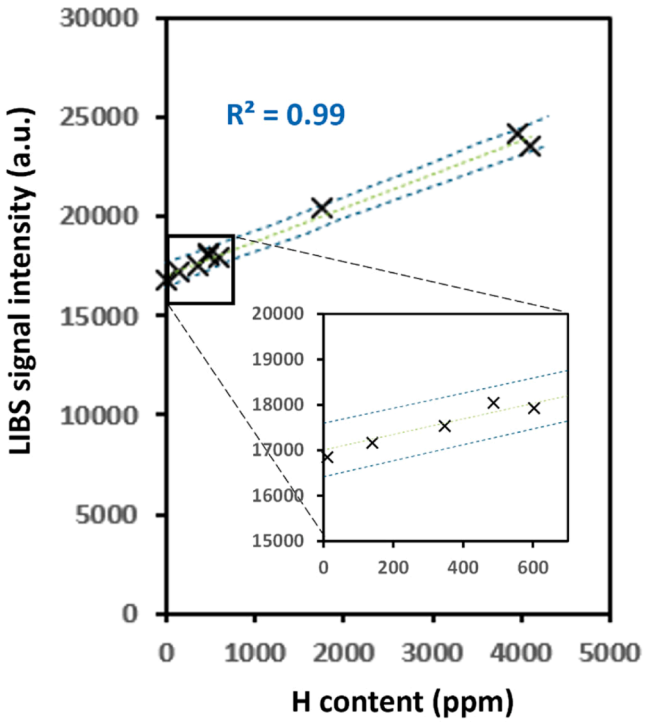


Fig. 7. Calibration model for Hydrogen LIBS quantitative measurement.

indicate that matrix effects remain limited for the investigated Zr alloys and that a common calibration approach can be applied within the framework of the present experimental configuration and concentration range. Under the present instrumental configuration and measurement protocol, the use of a direct hydrogen signal without additional normalization on Zr emission lines was therefore sufficient to obtain robust quantitative measurements.

4.4. Control of ambient hydrogen contribution

One of the major limitations of hydrogen analysis by LIBS arises from the contribution of hydrogen originating from ambient air and surface-adsorbed moisture. During plasma formation, water vapor molecules present in the surrounding atmosphere may dissociate and contribute to the H I 656.28 nm emission line, leading to a systematic background signal independent of the actual hydrogen content of the sample. To minimize this effect, local plasma inerting was optimized by varying the argon flow rate between 0.8 and 1.2 L/min using a calibrated flow meter. Results indicated that an optimal balance between plasma confinement and minimal turbulence was achieved at 1.0 L/min, for which the hydrogen signal exhibited maximum stability and signal-to-noise ratio. Furthermore, all measurements were carried out in a climate-controlled laboratory with regulated temperature and humidity. This contributes to maintaining stable ambient conditions throughout the study and helps limit variations in the atmospheric hydrogen contribution.

Despite localized inerting and climate-controlled conditions, a residual hydrogen contribution remains observable, resulting in a constant offset in the calibration curve. However, the linearity of the response over the investigated concentration range demonstrates that this contribution behaves as a stable systematic component. These results indicate that complete elimination of atmospheric hydrogen is not strictly required, as long as its contribution is stable and properly accounted for in the calibration strategy. Provided that calibration is performed under identical experimental conditions, the established calibration remains robust and reliable, which means that quantitative hydrogen determination remains valid.

The non-zero intercept of the calibration curve (cf. Fig. 7), however, makes it difficult to accurately determine the instrument's limit of detection (LoD). Indeed, it is difficult to establish whether the signal observed at the lowest concentration (12 wppm) arises solely from the ambient atmosphere. Nevertheless, a clear increase in the hydrogen signal is observed at the next concentration level (120 wppm), demonstrating that hydrogen can be reliably detected well below this concentration. The LoD is therefore expected to be below 100 wppm, most likely on the order of a few tens of wppm. Furthermore, the limit of quantification (LoQ) was estimated at 211 wppm using the confidence hyperbola approach (95% confidence level), further demonstrating the excellent analytical figures of merit achieved with this methodology.

4.5. Hydrogen quantitative imaging

The experimental conditions for LIBS measurements being optimized, a hydrogen map was performed on two $M5_{Framatome}$ samples with heterogenous hydrogen distribution. As mentioned in 3.3, samples were exposed to steam at 1200 °C in conditions leading to secondary hydriding [27]. Map size was defined as a matrix of 2100 × 96 points, corresponding to an analyzed area of 25.2 × 1.1 mm^2 (stage displacement step of 12 μm).

The lateral step size of 12 μm used in this study corresponds to the practical spatial resolution limit under the present instrumental conditions. This value was selected to prevent crater overlap between successive laser shots, which could otherwise induce cumulative thermal effects and increase shot-to-shot variability. Finally considering the ablation depth per pulse (~8 μm) and the absence of significant crater overlap, the measured signal can be attributed to a well-defined interaction volume, enabling reliable micrometer-scale spatial mapping. It should therefore be noted that the reported 12 μm spatial resolution represents the effective analytical resolution achievable while maintaining signal stability and quantitative reliability. Further reduction of the step size would require adaptation of laser energy and focusing conditions to preserve crater independence and plasma reproducibility. A small edge effect at the sample borders due to embedding resin is also observed, which could be improved in future studies by exploring metallic embedding materials.

Hydrogen maps, presented in Fig. 8, highlight the heterogeneous hydrogen distribution in the cladding wall thickness and in the axial direction. This heterogeneity reflects the material behavior during oxidation, as some regions absorb more hydrogen than others. This heterogeneous distribution is related to the partition of hydrogen between the ZrO_2, αZr(O) and βZr phases growing during the oxidation stage.

The microstructure observed after a high temperature steam oxidation and water quenching is illustrated in Fig. 9. The optical image is presented along with an oxygen map obtained by EPMA in the same region of the sample where the LIBS hydrogen map was performed. EPMA oxygen maps show high oxygen content areas where hydrogen is expected to be low, and the LIBS hydrogen map complements this information, demonstrating phase-dependent hydrogen distribution.

Hydrogen is a β-gene element and is expected to be concentrated in the prior-β phase and thus only a few tenths of wppm of hydrogen are expected in ZrO_2 and αZr(O) [7,34]. Indeed, the hydrogen maps show that very little hydrogen is measured in ZrO_2 and αZr(O). In the prior-β phase, the hydrogen concentration is rather inhomogeneous, with as much as 3000 wppm, in the region where the prior-β phase thickness is reduced, i.e. where double side steam oxidation occurred.

So, the α- and β-gene characteristics of oxygen and hydrogen respectively are clearly evidenced in Fig. 9.

4.6. Validation with neutron imaging

For comparison with NI and validation of the method, the hydrogen measurements obtained through LIBS analysis were used to construct an

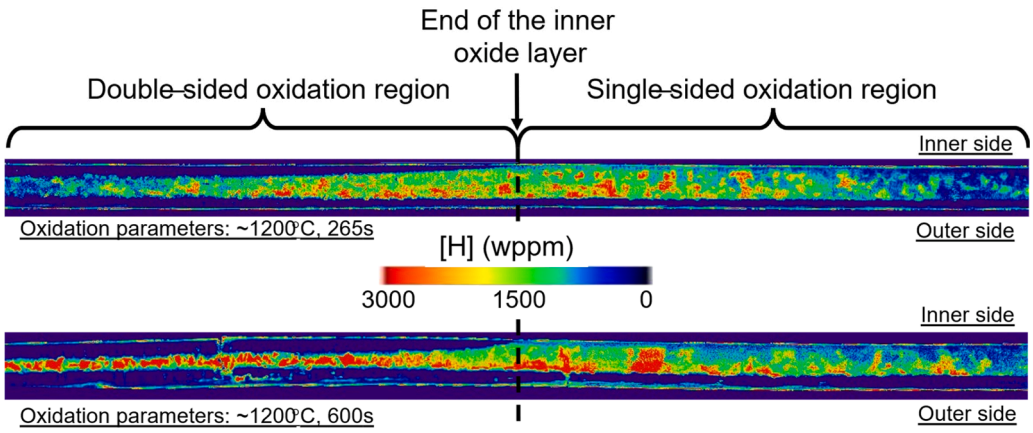


Fig. 8. LIBS hydrogen maps of $M5_{Framatome}$ oxidized under steam at 1200 °C.

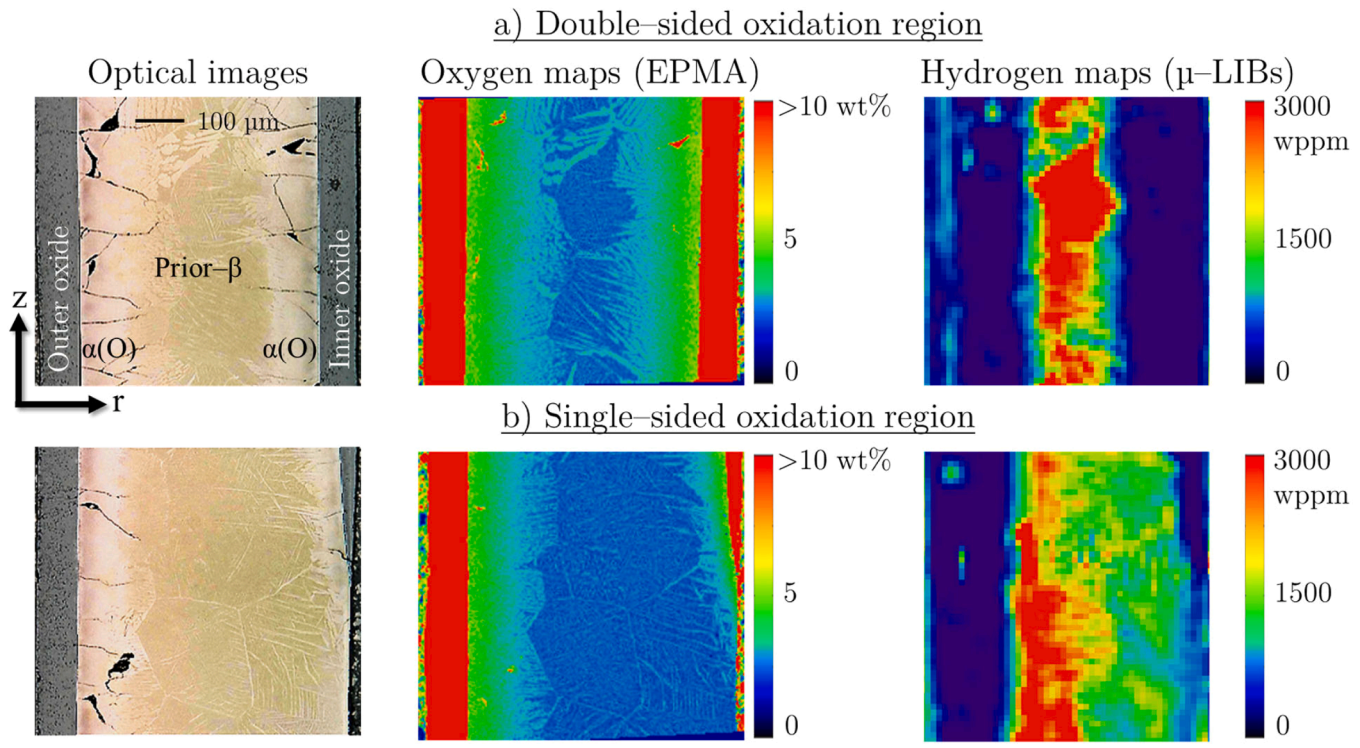


Fig. 9. Optical images, oxygen maps from EPMA and hydrogen maps from LIBS for the sample oxidized at 1200 °C under steam for 600 s.

average axial hydrogen profile over the analyzed region. The average axial profile was determined using the LIBS maps by drawing a Region Of Interest (ROI) made of a rectangular box which covers the entire cladding thickness including the oxide layers. For consistency with NI, the ROI includes the oxide layers in the determination of the average hydrogen content, although the LIBS signal is not calibrated in the oxide layer. However, the hydrogen content in the oxide is expected to be low [7,34]. The map size achieved with the LIBS analysis was long enough (25 mm) to derive axial hydrogen distribution profiles comparable to NI hydrogen profiles.

LIBS and NI were calibrated with different hydrogen standards prepared as mentioned in 3.1 [35].

Both hydrogen axial profiles are in good agreement in terms of hydrogen peak position and hydrogen amount, although there is slight difference on the side of the peak for strip n°1 and at the maximum of the peak for strip n°2 (Fig. 10). The comparison with NI, which is the reference method for hydrogen measurements, demonstrates that the LIBS protocol, which was developed, is valid for accurately measuring hydrogen profiles in zirconium alloys.

In addition, LIBS provides complementary information by offering local measurements through the wall thickness of cladding that are not accessible with the NI measurements performed. This complementary information shows that the local hydrogen content can reach up to 3000 wppm, whereas the average hydrogen content across the wall thickness does not exceed 2000 wppm.

5. Conclusions

Hydrogen is one of the most challenging elements to quantify and spatially map in solid materials due to its low atomic number, high mobility, and sensitivity to environmental contamination. This work demonstrates that, despite these challenges, Laser-Induced Breakdown Spectroscopy (LIBS) can provide reliable and quantitative hydrogen measurements in zirconium-based nuclear fuel claddings when

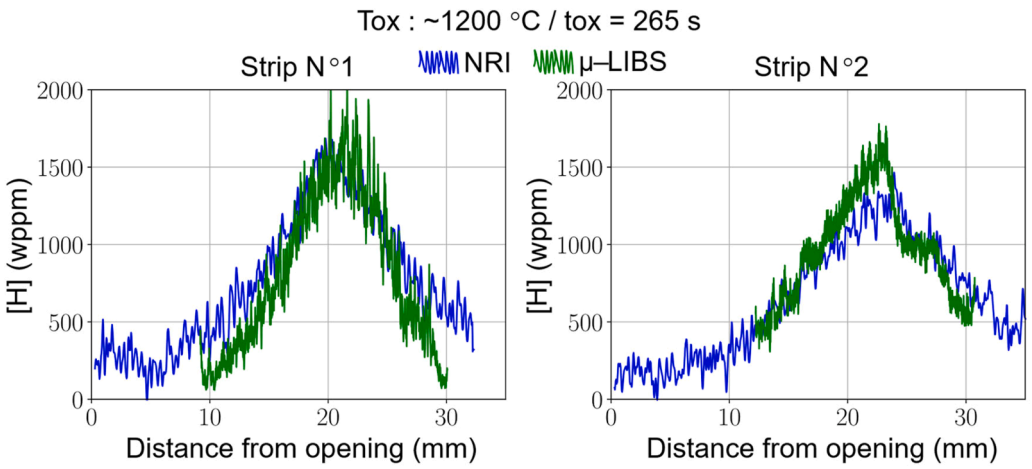


Fig. 10. Comparison of the hydrogen profiles obtained from the LIBS hydrogen maps and from NI after steam oxidation at 1200 °C for 265 s.

appropriate control of sample preparation, instrumental stability, and calibration procedures is achieved.

A complete methodology was developed and evaluated, including optimization of sample preparation, assessment of measurement repeatability and long-term reproducibility, investigation of matrix effects, and evaluation of ambient hydrogen contribution. The resulting calibration curve exhibited excellent linearity over the investigated concentration range (12–4100 wppm), with a detection limit below 100 wppm. Although a constant offset attributable to residual atmospheric hydrogen was observed, its stability across all standards demonstrated that this contribution behaves as a systematic constant term and does not prevent quantitative analysis when appropriate calibration is applied.

The use of two industrial zirconium alloy grades (Zry-4 and $M5_{Framatome}$) further demonstrated the robustness of the proposed approach. Limited matrix effects were observed under the experimental conditions investigated, supporting the applicability of a common calibration strategy across both alloy families and reinforcing the industrial relevance of the methodology.

Comparison with neutron imaging measurements demonstrated excellent agreement in both hydrogen concentration and spatial distribution, validating the proposed approach. In addition to providing quantitative information, LIBS offers complementary insights through its ability to resolve local hydrogen variations within the cladding wall thickness, revealing concentration gradients and localized hydrogen accumulation that are not accessible through bulk measurements alone. Overall, these results establish LIBS as a practical, accessible, and quantitative technique for hydrogen mapping in zirconium alloys. The methodology developed in this work enables rapid local hydrogen mapping at acquisition rates up to 100 Hz, with a spatial resolution of 12 µm and a detection limit below 100 wppm, making it particularly attractive for large-area characterization (up to 20 mm in length) and industrial applications.

Future developments will focus on extending the methodology toward high-resolution µ-LIBS configurations, with the objective of accessing hydrogen heterogeneities at the microstructural scale. Such developments would be particularly valuable for investigating hydrogen localization within prior-β regions and near αZr(O) interfaces, where hydrogen redistribution is closely linked to oxidation-induced phase transformations. Further work will therefore be required to adapt the quantitative calibration strategy to high-resolution configurations and to evaluate repeatability, reproducibility, matrix effects and detection limits under these conditions.

In addition, implementing the measurements in a fully controlled atmosphere chamber would make it possible to precisely regulate the ambient gas composition and humidity, thereby minimizing the contribution of atmospheric hydrogen and further improving the accuracy, sensitivity, and reliability of hydrogen quantification.

In this perspective, simultaneous oxygen analysis by LIBS represents a particularly important next step and a natural extension of the present methodology. Indeed, oxygen is a key element for understanding oxidation-induced phase transformations in zirconium alloys, as its distribution is directly related to the formation of ZrO_2 and αZr(O) regions and to the evolution of prior-β microstructures. Providing rapid, spatial-resolved elemental information with limited sample preparation, LIBS appears as a promising candidate for oxygen mapping in these metallic materials. Such a capability to map hydrogen and oxygen within the same measurement and over the same analyzed area would represent a significant advantage over complementary techniques such as ERDA or neutron imaging, which generally rely on separate analyzes for hydrogen and oxygen. Coupled with further progress in spatial resolution, combined hydrogen and oxygen LIBS imaging could pave the way toward phase-scale hydrogen quantification within prior-β and αZr(O) microstructural features, opening new opportunities for correlating hydrogen distribution with phase transformations, oxygen content and local degradation mechanisms.

More broadly, multi-element capability of LIBS also offers promising perspectives for the simultaneous detection of additional alloying or degradation-related elements, such as chromium, which is of particular interest for the characterization of chromium-coated claddings. This would enable simultaneous monitoring of coating integrity together with hydrogen and oxygen distribution. Such multi-element information could help relate hydrogen, chromium and oxygen distributions to local microstructural evolution, oxidation processes and elemental redistribution in nuclear materials, thereby strengthening the role of LIBS as a complementary tool for studying coupled chemical and microstructural changes in Zirconium alloys.

CRediT authorship contribution statement

S. Guilbert: Conceptualization, Methodology, Investigation, Formal analysis, Validation, Writing – original draft, Supervision. **L. Jolivet:** Conceptualization, Methodology, Investigation, Formal analysis, Validation, Writing – original draft, Supervision. **A.M. Kpemou:** Investigation, Formal analysis, Writing – review & editing. **V. Motto-Ros:** Methodology, Writing – review & editing. **M. Grosse:** Investigation, Formal analysis, Writing – review & editing. **F. Trichard:** Methodology, Writing – review & editing.

Declaration of competing interest

The authors declare that they have no known competing financial

interests or personal relationships that could have appeared to influence the work reported in this paper.

Acknowledgements

The neutron radiography experiments were performed at the ICON facility at the Swiss neutron source SINQ. The authors would like to thank Mrs Sarah Weick from KIT for her contribution to the neutron radiography measurements.

Data availability

Research Link Provided
Hydrogen quantitative mapping by LIBS (Original data) (ORCID)

References

[1] A.T. Motta, et al., Hydrogen in zirconium alloys: a review, », J. Nucl. Mater. 518 (2019) 440–460, https://doi.org/10.1016/j.jnucmat.2019.02.042. mai.
[2] M. Grosse, E. Lehmann, P. Vontobel, M. Steinbrueck, et al., Quantitative determination of absorbed hydrogen in oxidised Zircaloy by means of neutron radiography, », Nucl. Instrum. Methods Phys. Res., Sect. A 566 (2) (2006) 739–745, https://doi.org/10.1016/j.nima.2006.06.038. n°oct.
[3] M. Grosse, et al., Neutron imaging investigations of the secondary hydriding of nuclear fuel cladding alloys during loss of coolant accidents, », Phys. Procedia 69 (2015) 436–444, https://doi.org/10.1016/j.phpro.2015.07.061.
[4] C. Raepsaet, P. Bossis, D. Hamon, J.L. Béchade, J.C. Brachet, et al., Quantification and local distribution of hydrogen within Zircaloy-4 PWR nuclear fuel cladding tubes at the nuclear microprobe of the Pierre Süe Laboratory from μ-ERDA, », Nuclear Instrum. Methods Phys. Res. Section B: Beam Inter. Mater. Atoms 266 (10) (2008) 2424–2428, https://doi.org/10.1016/j.nimb.2008.03.041. n°mai.
[5] Z. Weiss, Analysis of hydrogen in inorganic materials and coatings: a critical review, », Hydrogen 2 (2) (2021) 225–245, https://doi.org/10.3390/hydrogen2020012. n°.
[6] M. Grosse, N. Kardjilov, et al., Which resolution can be achieved in practice in neutron imaging experiments? – A general view and application on the Zr - ZrH_2 and ZrO_2 - ZrN systems, », Phys. Procedia 88 (2017) 266–274, https://doi.org/10.1016/j.phpro.2017.06.037. janv..
[7] J.-C. Brachet, et al., Study of secondary hydriding at high temperature in zirconium based nuclear fuel cladding tubes by coupling information from neutron radiography/tomography, electron probe micro analysis, micro elastic recoil detection analysis and laser induced breakdown spectroscopy microprobe, », J. Nucl. Mater. 488 (2017) 267–286, https://doi.org/10.1016/j.jnucmat.2017.03.009. mai.
[8] M. Grosse, M. van den Berg, C. Goulet, A. Kaestner, et al., In-situ investigation of hydrogen diffusion in Zircaloy-4 by means of neutron radiography, », in: présented at 5th European Conference on Neutron Scattering, Prague, Czech Republic, 2012.
[9] et al. M. Grosse, M. van den Berg, C. Goulet, E. Lehmann, B. Schillinger, In-situ neutron radiography investigations of hydrogen diffusion and absorption in zirconium alloys, » Nucl. Instrum. Methods Phys. Res., Sect. A 651 (1) (2011) 253–257, https://doi.org/10.1016/j.nima.2010.12.070. n°sept
[10] M. Wilde, K. Fukutani, et al., Hydrogen detection near surfaces and shallow interfaces with resonant nuclear reaction analysis, », Surf. Sci. Rep. 69 (4) (2014) 196–295, https://doi.org/10.1016/j.surfrep.2014.08.002. n°déc..
[11] N. Mine, S. Portier, M. Martin, et al., Imaging and hydrogen analysis by SIMS in zirconium alloy cladding: a dual ion beam approach, », Surf. Interface Anal. 46 (S1) (2014) 249–252, https://doi.org/10.1002/sia.5466. n°nov.
[12] «edited by M. Grasserbauer, «, in: J.C. Vickerman (Ed.), Principles and Applications of SIMS: Secondary ion Mass Spectroscopy Principles and Applications, Principles and Applications of SIMS: Secondary ion Mass Spectroscopy Principles and Applications, 9, Clarendon Press, Oxford, 1990, p. IX, https://doi.org/10.1016/0165-9936(90)87048-Q. edited by1989 £45.00 (xiii + 341 pages), ISBN: 0-198556-25-X », *TrAC Trends in Analytical Chemistry*n°juin.
[13] P.P. Michałowski, Secondary ion mass spectrometry measurements with a large scale-to-resolution ratio, », Appl. Surf. Sci. 702 (2025) 163272 https://doi.org/10.1016/j.apsusc.2025.163272. sept.
[14] D. Rhede, M. Wiedenbeck, et al., SIMS quantification of very low hydrogen contents, », Appl. Surf. Sci. 252 (19) (2006) 7152–7154, https://doi.org/10.1016/j.apsusc.2006.02.245. n°juill.
[15] I. Okseniuk, D. Shevchenko, et al., SIMS studies of hydrogen interaction with the TiFe alloy surface: hydrogen influence on secondary ion yields, », Surf. Sci. 716 (2022) 121963 https://doi.org/10.1016/j.susc.2021.121963. févr.
[16] J. Fernandes, et al., Looking inside electrodes at the microscale with LIBS: li distribution, », Spectrochim. Acta Part B: Atomic Spectrosc. 221 (2024) 107047 https://doi.org/10.1016/j.sab.2024.107047. nov.
[17] C. Marina-Montes, V. Motto-Ros, L.V. Pérez-Arribas, J. Anzano, M. Millán-Martínez, J.O. Cáceres, et al., Aerosol analysis by micro laser-induced breakdown spectroscopy: a new protocol for particulate matter characterization in filters, », Anal. Chim. Acta 1181 (2021) 338947 https://doi.org/10.1016/j.aca.2021.338947. oct.
[18] B. Busser, et al., Characterization of foreign materials in paraffin-embedded pathological specimens using in situ multi-elemental imaging with laser spectroscopy, », Modern Pathol. 31 (3) (2018) 378–384, https://doi.org/10.1038/modpathol.2017.152. n°mars.
[19] F. Trichard, et al., Imaging of alumina supports by laser-induced breakdown spectroscopy: a new tool to understand the diffusion of trace metal impurities, », J. Catal. 363 (2018) 183–190, https://doi.org/10.1016/j.jcat.2018.04.013. juill.
[20] M. Pardede, et al., Comparative study of laser-induced plasma emission of hydrogen from zircaloy-2 samples in atmospheric and low pressure ambient helium gas, », Appl. Phys. B 89 (2) (2007) 291–298, https://doi.org/10.1007/s00340-007-2780-x. n°nov.
[21] E.J. Kautz, E.C.E. Rönnebro, A. Devaraj, D.J. Senor, S.S. Harilal, et al., Detection of hydrogen isotopes in Zircaloy-4 via femtosecond LIBS, », J. Anal. At. Spectrom. 36 (6) (2021) 1217–1227, https://doi.org/10.1039/D1JA00034A. n°.
[22] M. Ramli, et al., Quantitative hydrogen analysis of Zircaloy-4 in laser-induced breakdown spectroscopy with ambient helium gas, », Appl. Opt. 46 (34) (2007) 8298, https://doi.org/10.1364/AO.46.008298. n°déc.
[23] K.H. Kurniawan, et al., Quantitative hydrogen analysis of Zircaloy-4 using low-pressure laser plasma technique, », Anal. Chem. 79 (7) (2007) 2703–2707, https://doi.org/10.1021/ac061713o. n°avr.
[24] D.A. Cremers, L.J. Radziemski, et al., Handbook of Laser-INduced Breakdown Spectroscopy, Wiley&Sons, Ltd., New-York, 2006.
[25] W.A. Miziolek, V. Palleschi, I. Schechter, et al., Laser-Induced Breakdown Spectroscopy (LIBS), 1st Edition, Cambridge University Press, 2008.
[26] D.W. Hahn, N. Omenetto, et al., Laser-induced breakdown spectroscopy (LIBS), part I: review of basic diagnostics and plasma-particle interactions: still-challenging issues within the analytical plasma community, », Appl. Spectrosc. (2010) 335–366.
[27] A.M. Kpemou, et al., A new approach to investigate secondary hydriding phenomenon on $M5_{Framatome}$ clads under high–temperature LOCA conditions, », J. Nucl. Mater. 603 (2025) 155462 https://doi.org/10.1016/j.jnucmat.2024.155462.
[28] M. Grosse, M. Steinbrueck, E. Lehmann, P. Vontobel, et al., Kinetics of hydrogen absorption and release in zirconium alloys during steam oxidation, », Oxid. Met. 70 (3) (2008) 149–162, https://doi.org/10.1007/s11085-008-9113-2. n°oct.
[29] E.H. Lehmann, P. Vontobel, A. Hermann, et al., Non-destructive analysis of nuclear fuel by means of thermal and cold neutrons, », Nucl. Instrum. Methods Phys. Res., Sect. A 515 (3) (2003) 745–759, https://doi.org/10.1016/j.nima.2003.07.059. n°déc.
[30] R. Yasuda, M. Matsubayashi, M. Nakata, K. Harada, et al., Application of neutron radiography for estimating concentration and distribution of hydrogen in Zircaloy cladding tubes, », J. Nucl. Mater. 302 (2) (2002) 156–164, https://doi.org/10.1016/S0022-3115(02)00778-X. n°avr.
[31] T. Smith, H. Bilheux, H. Ray, J.-C. Bilheux, Y. Yan, et al., High resolution neutron radiography and tomography of hydrided Zircaloy-4 cladding materials, », Phys. Procedia 69 (2015) 478–482, https://doi.org/10.1016/j.phpro.2015.07.067. janv.
[32] C. Fabre, et al., Elemental imaging by laser-induced breakdown spectroscopy for the geological characterization of minerals, », J. Anal. At. Spectrom. (2018) 1345–1353, 2 juillet.
[33] V. Motto-Ros, S. Moncayo, F. Trichard, F. Pelascini, et al., Investigation of signal extraction in the frame of laser induced breakdown spectroscopy imaging, », Spectrochim. Acta Part B: Atomic Spectrosc. 155 (2019) 127–133, https://doi.org/10.1016/j.sab.2019.04.004. mai.
[34] K. Park, D.R. Olander, et al., Hydrogen dissolution in and release from nonmetals: III, tetragonal zirconia, », J. Am. Ceram. Soc. 74 (1) (1991) 72–77, https://doi.org/10.1111/j.1151-2916.1991.tb07299.x. n°janv..
[35] A.M. Kpemou, et al., Experimental study of secondary hydriding during a LOCA transient, ». TOPFUEL 2024, Grenoble, France, 2024. oct..